Design of Anisotropic Pneumatic Artificial Muscles and Their Applications to Soft Wearable Devices for Text Neck Symptoms

Hojoong Kim, Hyuntai Park, and Jongwoo Kim, *Member, IEEE*, Kyu-Jin Cho, *Member, IEEE*, and Yong-Lae Park, *Member, IEEE*

***Abstract*—Pneumatic artificial muscles (PAMs) are frequently used actuators in soft robotics due to their structural flexibility. They are generally characterized by the tensile force due to the axial contraction and the radial force with volume expansion. To date, most applications of PAMs have utilized axial contractions. In contrast, we propose a novel way to control radial expansions of particular PAMs using anisotropic behaviors. PAMs generally consist of a cylindrical rubber bladder that expands with injection of air and multiple flexible but inextensible strings or mesh that surround the bladder to generate axial contraction force. We propose methods of generating radial expansion force in two ways. One is to control the spatial density of the strings that hold the bladder, and the other is to give asymmetric patterns directly to the bladder for geometrical anisotropy. To evaluate the performance of the actuators, soft sensors made of a hyperelastic material and a liquid conductor were attached to the PAMs for measuring local strains and pressures of the PAMs. We also suggest use of the proposed PAMs to a wearable therapeutic device for treating text neck symptoms as an application. The PAMs were used to exert a pressure to the back of the neck to recover the original spinal alignment from the deformed shape.**

I. Introduction

Pneumatic artificial muscles (PAMs) are a type of actuators powered by compressed air. They are frequently used in soft robots, since they do not require rigid parts, such as mechanical joints and fasteners (i.e. bolts and nuts), while generating linear or bending forces. McKibben-type PAMs are one of the most popular forms that consist of a cylindrical bladder made of silicone rubber wrapped with a mesh structure or a bundle of cords made of inextensible materials [1]. When the rubber bladder is loaded with air, it inflates radially but contracts axially. While traditional PAMs have mostly been used for their axial tensile force, their radial expansion has not been taken into account in typical robotic systems [2, 3]. Similar to biological muscles in principle, PAMs have been applied to various soft robotic systems. However, the current applications of PAMs may not be the best solution when it comes to wearable device for biomedical purposes, especially in orthopedic devices. One of the basic principles of orthotherapy is compressing the human body while keeping contact [4]. In this case, PAMs are effective on delivering and/or maintaining the compression through its pressurized body. However, conventional PAMs have a limitation of control in terms of the orientation of expansion, resulting in an inefficacy when used for orthopedic therapies.

The goal of this study is to design and fabricate an anisotropic PAM (APAM) focused on its radial expansion that can be reliably controlled. The idea in our design is to control and utilize the radial expansion of the PAM by changing the geometry from traditional McKibben-type PAMs. We propose two types of design. One is an air bladder with asymmetrically embedded reinforcement strings. The area with fewer strings makes larger expansion than that with more strings, resulting in anisotropic bladder expansion (i.e. bending) in spite of the uniform internal air pressure (Type 1). The other is a bladder with multiple narrow grooves perpendicular to the length of the bladder only on one side, making a larger surface area, resulting in bending (Type 2), which is similar to PneuNets [5].

We also propose applications of the above APAMs to an orthopedic therapeutic wearable device for treating neck diseases, specifically focusing on text neck symptoms. Existing treatment includes pressurizing the back of the neck to recover the original curved shape of the cervical vertebral. Since the APAMs is capable of selectively deliver mechanical pressure to a target area, they are expected to help alleviating the symptoms if properly installed.

Design and fabrication of the two types of PAMs and their applications to a wearable device for text neck symptoms are described in this paper. The evaluation of the muscles and the wearable devices are also discussed.

II. Methodologies

The main components of APAMs are an elastomer bladder (for both types) and non-stretchable strings around the bladder (only for Type 1). The bladders are made of silicone elastomer (Ecoflex-0030, Smooth-on). Liquid elastomer is poured into a mold and cured at 65℃. For comparison, the design parameters of the rubber bladder were selected equally. The thickness and the length are 4 mm and 200 mm, respectively. The dimensions of the cross-sections of both types are also the same.

This work was supported in part by the Undergraduate Research Program (URP) at Seoul National University, and in part by the National Research Foundation of Korea (NRF) Grant funded by the Korean Government (MSIP) (NRF-2016R1A5A1938472).

H. Kim and H. Park are with the Department of Mechanical and Aerospace Engineering, Seoul National University, Seoul, 08826 Korea (e-mail: khj2195@snu.ac.kr, qkrgusxo0927@snu.ac.kr). H. Kim and H. Park contributed equally to this work.

J. Kim and K. Cho are with Biorobotics Laboratory, the Department of Mechanical and Aerospace Engineering, Seoul National University, Seoul, 08826 Korea (e-mail: kimjongwoo1988@gmail.com).

Y.-L Park is with the Department of Mechanical and Aerospace Engineering, Seoul National University, Seoul, 08826 Korea, and also with the Robotics Institute, Carnegie Mellon University, Pittsburgh, 15213 (e-mail: ylpark@snu.ac.kr).

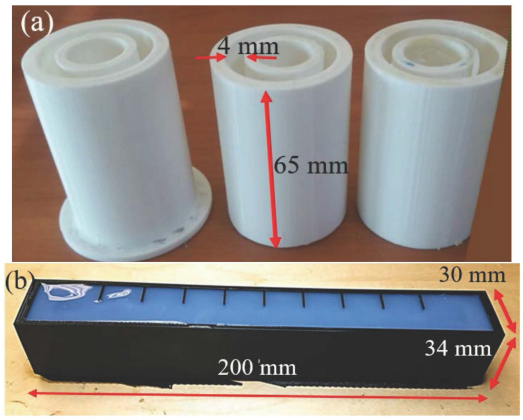

Figure 1. Mold of PAMs. (a) Mold of Type 1 APAM. (b) Mold of Type 2 APAM.

Type 1 APAM was fabricated with three elastomer tubes combined in series into a long single cylindrical bladder. Molds for the tubes are show in Fig. 1(a). Liquid-state silicone was used as an adhesive for bonding the three tubes. Both ends of the cylinder were sealed with additional silicone and covered with solid caps. Once the polymer cured, 12 flexible but inextensible strings were equidistantly aligned around the bladder [6, 7]. Finally, the expansion surface is determined by removing a couple of strings on one side. Type 2 APAM is cast with a single mold, as shown in Fig. 1(b). The groove pattern is made in the mold to increase the surface area of one side. Fig. 2 shows the behaviors of the two APAMs. In both cases, the PAMs expand upwards and bend downwards.

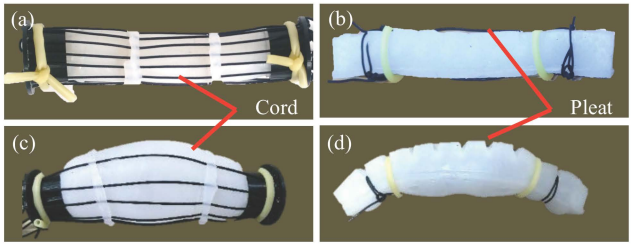

Figure 2. (a) Type 1 APAM (unloaded). (b) Type 2 APAM (unloaded). (c) Type 1 APAM (loaded). (d) Type 2 APAM (loaded).

In order to measure the expansion of the PAMs, soft sensors were built and integrated with the PAMs using the same material of the bladders. The soft sensor has a serpentine microchannel filled with a liquid metal (eutectic gallium-indium, eGaIn), as shown in Fig. 3. The microchannel changes its electrical resistance in response to strain and/or external contact pressure inputs [8]. To read sensor data, a microcontroller (Arduino Uno, SparkFun) circuit was built (Fig. 4). Adapting input resistance of amplifier (R_G) to 10 kΩ and applying Eq. (1), we set the gain to 5.94. Then, the resistance of the soft sensor can be obtained from Eq. (2), where i and x refer to current flowing through sensor and output variable from Arduino respectively. When the sensors are pressurized or elongated, the outcome value of the resistance changes accordingly [9, 10].

$$G = 49.4/R_G + 1 \quad (1)$$

$$R = \frac{3.3Gx}{1024i} \quad (2)$$

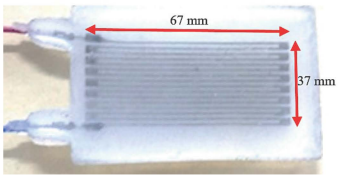

Figure 3. Soft sensor.

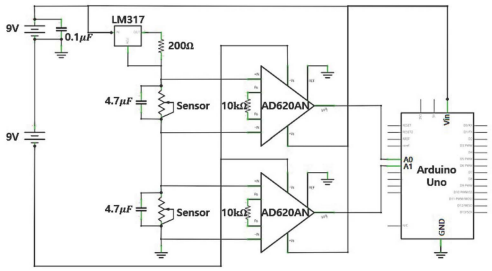

Figure 4. Circuit for soft sensor measurement

Although the soft sensor is sensitive to both strain and pressure, the sensor gives only one type of output, electrical resistance. To characterize the strain and pressure responses, the soft sensor was tested with varied strains and pressures, as shown in Fig. 5. The result, in Fig. 5(a), show that the sensor is linear with strain input up to 45% strain, and the gauge factor is 1.605. Contact pressure was measured by applying a load with a known area with different strain level, and the data was exponentially fitted, as shown in Fig. 5(b). For evaluating the performance of the PAMs, soft sensors were attached to the PAMs and measured resistance changes. We attached the soft sensors to three areas of Type 1 PAM, top, bottom and side, and two areas of Type 2 PAM, top and bottom, as shown in Fig. 6.

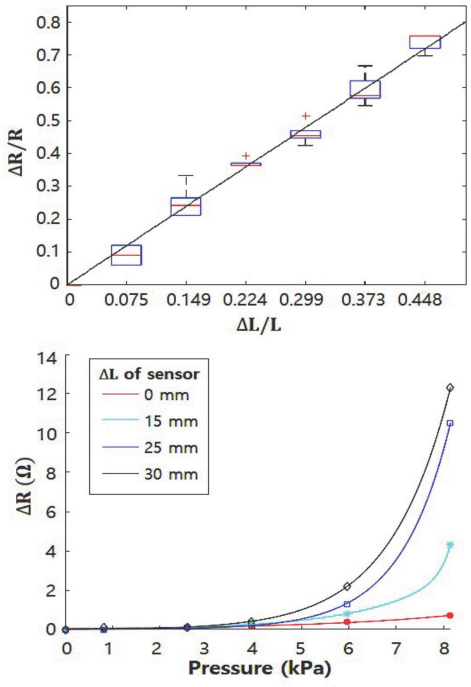

Figure 5. Sensor calibration: Resistance-strain characteristic under no-pressure condition (top). Resistance-pressure characteristic under various values of strain (bottom).

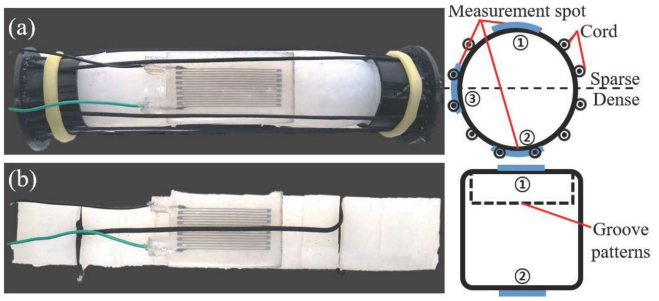

Figure 6. APAMs with sensor attached and cross-section diagram. (a) Type 1 with three sensor locations. (b) Type 2 with two sensor locations.

III. Results

Radial expansion of the APAMs can be estimated from the soft sensor based on the result shown in Fig. 5. In this case, other types of deformation, such as bending and twisting, were not considered since they did not significantly influence the overall shape. We compared the expansion of the APAMs with that of isotropic PAM, a control group. The experimental result from the isotropic PAM is shown in Table I. The isotropic PAM expanded by 5 mm in its length. During this expansion, the estimated pressure was approximately 57.4 kPa from the soft sensor.

Table I. Sensor data of isotropic PAM

State	Resistance (Ω)	Length (mm)
Uninflated	3.3	67.0
Inflated	11.9	72.0

Before repeating the same expansion test with APAMs, we visually examined the anisotropy of the APAMs. The geometric profiles of the expanded APAMs were assumed to be arcs with maximum and minimum expansion areas, as indicated in Fig. 7. S and h are defined to be length between the two ends of the APAM and the height of the expanded area, respectively, and r is the radius of curvature, as shown in Fig. 8. Then, we can find S, h, and r from Equations (3) and (4), as shown in Table. II. Both types of the APAMs showed significant difference between the maximum and minimum values for curvature radii, showing clear anisotropic deformation. During the expansion, the resistance changes of the soft sensors attached to the PAMs were measured, as shown in Table III.

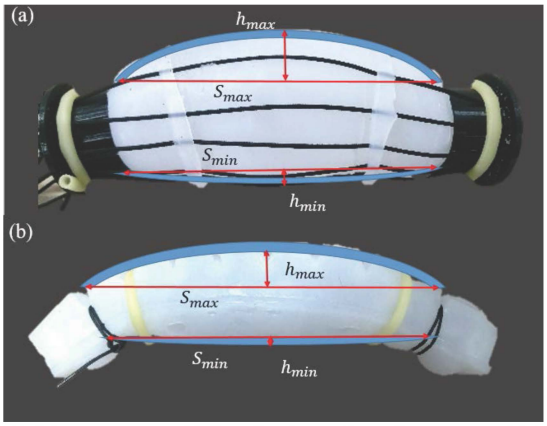

Figure 7. Measurement guideline for the radius of curvature. (a) Type 1 APAM. (b) Type 2 APAM.

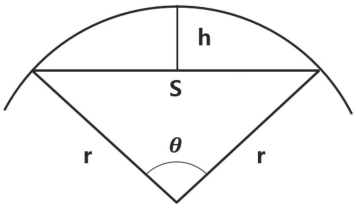

Figure 8. Diagram of radius curvature.

$$\begin{cases} S = 2r\sin(\theta/2) \\ h = r\{1-\cos(\theta/2)\} \end{cases} \quad (3)$$

Then, the radius of curvature r is

$$r = \frac{S}{2\sin\{2tan^{-1}(2h/S)\}}. \quad (4)$$

Table II. The radius of curvature of APAMs

Data (mm)	Type 1 Locations		Type 2 Locations		Isotropic PAM
	1	*2*	*1*	*2*	
S	150.0	145.0	167.0	150.0	157.0
h	35.0	6.0	20.0	3.0	12.0
r	97.9	441.0	184.3	939.0	262.8

Table III. Sensor and expansion result of APAMs

State		Type 1		Type 2	
		ΔR (Ω)	*ΔL (mm)*	*ΔR (Ω)*	*ΔL (mm)*
Uninflated		0.0	0.0	0.0	0.0
Inflated	Location 1	14.3	6.0	9.8	5.0
	Location 2	5.9	2.0	4.9	3.0
	Location 3	8.0	4.0	-	-

Finally, lateral expansions of the APAMs were evaluated with different pressure levels, as shown in Table IV. While pressure and elongation did not vary with the sensor locations in the isotropic PAM, the APAMs showed different sensor outputs with locations. In Type 1, measured pressures at the minimum and maximum inflation locations were approximately 51.0 kPa and 71.9 kPa, respectively. A negative correlation between pressure and radius curvature was derived. Especially, the pressure at location 1 where the highest inflation was observed turns out to be 25.4% larger than that of the isotropic PAM. This means that the APAM designs were effective for anisotropic lateral expansion. On the other hand, the result of Type 2 showed 61.4 kPa and 44.6 kPa at Locations region 1 and 2, respectively. The minimum pressure measured at Location 2 of Type 2 APAM was 23.3% smaller than that of the isotropic PAM, showing pressure-withholding effect.

Table IV. Correlation between curvature radius and pressure

Target of Measurement	Radius curvature (mm)	Pressure (kPa)
Type 1, r_{max}	97.9	71.9
Type 2, r_{max}	184.3	61.4
Isotropic PAM	262.8	57.4
Type 1, r_{min}	441.0	51.0
Type 2, r_{min}	939.0	44.6

IV. Discussion and Conclusion

We propose new designs of PAMs focused on anisotropic lateral inflation in this paper. In our designs, the primary orientation of radial expansion can be controlled. Although the radial expansion force of our APAMs is not as strong as the axial contraction force in general PAMs, it could be useful if reliably and effectively controlled. This type of force can be used to apply compressive force in some biomedical applications, making APAMs a useful tool to mechanically pressurize certain parts of the human body. Two design approaches were discussed in this paper.

The first approach is to place multiple strings asymmetrically around the stretchable bladder (Type 1). When the bladder inflates, the area with less strings expand more and generates radial expansion force. The advantage of this design is radial expansion while constraining the axial motion. However, the fabrication is relatively complicated due to the string alignment and placement process. This design was experimentally validated with experiments. Also, soft sensors were implemented to detect anisotropic expansion. Optimization of the configuration and distribution of the strings is an area of future research.

The second approach is to provide geometrical asymmetry directly to the bladder (Type 2). The bladder has multiple deep groove patterns to increase the surface only one side. The bladder looks like a straight rectangular bar without inflation. However, when inflated the side with groove patterns expands much more than the other flat side, consequently making anisotropic radial expansion. Although this design makes the fabrication process relatively simple since it does not require additional steps for embedding or placing other materials, such as strings or mesh, the radial expansion is not as large as that of Type 1, since the axial expansion is not physically constrained in this design. We also plan to optimize the number and the configuration of the groove patterns.

Finally, we implemented our actuators to an orthopedic wearable device for treating text neck symptoms, as suggested in [11]. The cervical spinal alignment of a typical text neck patient appears in Fig. 9(a). The directions of the external forces to be applied for the symptoms are shown in in Fig. 9(a). These forces are needed to recover the normal spinal alignment shown in Fig. 9(b) [12]. The force in the direction 2 requires application of pressure to a curved surface of the back of the neck. PAMs have an advantage in this case due to its conformability and softness, which may minimize discomfort on the neck. Also, it is easy to customize the size and the shape of the PAMs depending on users. Fig. 9(c) shows a prototype of our wearable device to treat text neck . The radial expansion compresses the back of the neck to align the spines. This design can customize the force and direction according to not only the physical variations from person to person but also the individual constant changes of the degrees of symptoms . To increase the wearability and functionality, we plan to optimize the pattern of rubber bladder and to use multiple PAMs together. Although the prototype is still conceptual, we expect that further investigations will improve the efficacy of the device and also broaden the scope of applications of PAMs to other biomedical wearable devices.

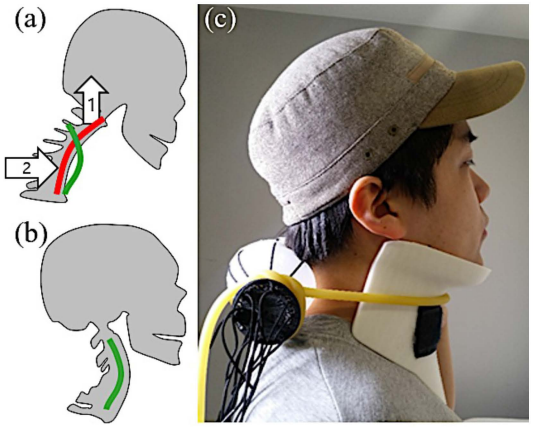

Figure 9. Skeletal arrangement of (a) a text neck patient and (b) a normal person. (c) Orthopedic wearable device using APAM type 1.

References

[1] G. K. Klute, J. M. Czerniecki, and B. Hannaford, "McKibben artificial muscles: pneumatic actuators with biomechanical intelligence," in *IEEE/ASME International Conf. on Advanced Intelligent Mechatronics,* pp. 221-226, 1999.

[2] B. Tondu, S. Ippolito, and J. Guiochet, "A seven-degrees-of-freedom robot-arm driven by pneumatic artificial muscles for humanoid robots," *The International Journal of Robotics Research*, Vol. 24, pp. 257-274, 2005.

[3] T. Noritsugu and T. Tanaka, "Application of rubber artificial muscle manipulator as a rehabilitation robot," *IEEE/ASME Trans. On Mechatronics*, Vol. 2, pp. 259-267, 1997

[4] T. Noritsugu, H. Yamamoto, D. Sasaki, and M. Takaiwa, "Wearable power assist device for hand grasping using pneumatic artificial rubber muscle," in *SICE Annual Conference,* Vol. 1, pp. 420-425, 2004.

[5] P. Polygerinos, S. Lyne, Z. Wang, L. F. Nicolini, B. Mosadegh, G. M. Whitesides, and C. J. Walsh, "Towards a soft pneumatic glove for hand rehabilitation," in *IEEE/RSJ International Conf. on Intelligent Robots and Systems*, pp. 1512-1517, 2013.

[6] K. Koter, L. Podsędkowski, and T. Szmechtyk, "Transversal Pneumatic Artificial Muscles," in *10th International Workshop on Robot Motion and Control (RoMoCo)*, pp. 235-239, 2015.

[7] T. Nakamura, N. Saga, and K. Yaegashi, "Development of a pneumatic artificial muscle based on biomechanical characteristics," in *IEEE International Conf. on Industrial Technology,* Vol. 2, pp. 729-734, 2003.

[8] Y.-L. Park, C. Majidi, R. Kramer, P. Berard, and R. J. Wood, "Hyperelastic pressure sensing with a liquid-embedded elastomer," *Journal of Micromechanics and Microengineering*, Vol. 20, No. 12, 125029 (6pp), 2010.

[9] Y.-L. Park, B.-r. Chen, and R. J. Wood, "Design and fabrication of soft artificial skin using embedded microchannels and liquid conductors," *IEEE Sensors Journal*, Vol. 12, pp. 2711-2718, 2012.

[10] J.-B. Chossat, Y.-L. Park, R. J. Wood, and V. Duchaine, "A soft strain sensor based on ionic and metal liquids," *IEEE Sensors Journal*, Vol.13, pp. 3405-3414, 2013.

[11] J. Lee, Y. Chee, J. Bae, H. Kim, and Y. Kim, "The Wearable Sensor System to Monitor the Head & Neck Posture in Daily Life," *Journal of Biomedical Engineering Research*, Vol.37, pp. 112-118, 2016.

[12] W. K. Oh, E. Lee, and B.-C. Shin, "Clinical effect of bong chuna manual therapy and acupuncture treatment for improving cervical curvature of turtle neck syndrome and measurement method of radiography", *J Oriental Rehab Med,* Vol.19, pp.113-124, 2009.